Monostatic and Bistatic Measurements of Metasurfaces on Anechoic Chamber and a Comparison with Electromagnetic Simulations

H. Fernández Álvarez, M.E. de Cos and F. Las-Heras
[1] Dept. Electrical Engineering, University of Oviedo, Gijón, Spain
fernandezhumberto@uniovi.es

***Abstract*— The paper will be focused on experimentally characterize a metasurface absorber under both a quasi-monostatic and a bistatic set-up configuration. The aim is to introduce most of the difficulties that a researcher may encounter, when characterizing this finite structure and compare them with the simulation, which assumes the metasurface as infinite. Moreover, the limitations of both the quasi-monostatic and bistatic measurements will be introduced, as well as a comparison between them. In addition, several guidelines to retrieve precise measurements are provided and applied to the presented set-ups. These recommendations will be of interest for many authors who want to experimentally characterize their metasurfaces. The latter will be corroborated through the high-quality and precise measurements obtained and shown throughout this paper.**

***Index Terms*—metasurface, monostatic measurement, bistatic measurement, metasurface absorber, angular stability.**

I. INTRODUCTION

Many papers have been devoted to analyze metasurfaces (MTS) only through electromagnetic simulations, either because the authors focus their work on improving some of the MTS properties (bandwidth, angular stability, multiresonance) [1]-[3] or they aim to develop an equivalent circuit model to properly predict the MTS behavior [4]-[5]. In addition, at optical frequencies it is fairly common to study the MTS in the same way, since the techniques needed to manufacture and measure the structures must be extremely precise and they are not available in any laboratory [6]. Consequently, there are not many contributions focused on evaluating the final finite MTS experimentally and even less in which a suitable explanation is provided. Indeed, most of the works just experimentally analyze the MTS behavior under normal incidence, even when it has been simulated under different polarizations and incidence angles [7]-[9].

When testing finite MTSs under different incidence angles, it is crucial to distinguish between monostatic and bistatic measurements. Monostatic measurements are conducted with the transmitting and receiving antennas in the same position, while the MTS is rotated. In the bistatic ones, the MTS remains static and the transmitting antenna is oriented in such a way that the incident wave impinges on the MTS, with the desired incidence angle, being the receiving one placed in the specular direction. The latter measurements are usually conducted using an arch measurement set-up [10] or other man made rudimentary set-ups [11]-[13]. However, the measurable distance of the latter set-ups is usually short and only small prototypes can be characterized under far-field conditions over a considerable frequency band. On the other hand, for characterizing the MTS under more controllable conditions, an anechoic chamber is employed. The latter is usually configured to measure antennas and hence, when metasurfaces are wanted to be analyzed inside them, a monostatic or quasi-monostatic measurement is usually conducted.

Some of the problems that arise when metasurfaces are wanted to be characterized under a monostatic or quasi-monostatic configuration have been shown in a previous paper [14], as well as guidelines to enhance the measurement precision. However, more accurate measurements can be obtained following new additional recommendations, which will be analyzed in this paper. Moreover, measurements conducted under a bistatic configuration in the same environment as in [14] and using the same metasurface absorber (MTA) will be also introduced. Furthermore, the limitations of measuring the angular stability on an anechoic chamber, using either a quasi-monostatic or bistatic set-up arrangement, are presented.

II. SIMULATION VERSUS MEASUREMENTS REGARDING ANGULAR STABILITY.

In order to avoid computational burden when simulating MTS, the structure is considered as infinite and hence, the Bloch-Floquet theorem can be applied [15]. Indeed, the simulated infinite MTS provides a really reliable approximation to the resonance frequency of the finite one, as long as proper dimensions are chosen for the latter. Under this consideration, the results of analyzing the MTS through monostatic and bistatic measurements are senseless, since its scattering pattern should be equal. Actually, these two characterizations may be considered as being analogous. Moreover, the simulation restrictions of infinite structures are significantly lesser than the ones of characterizing finite structures on an experimental environment, mainly due to scattering issues. In fact, when analyzing the angular stability

of finite MTS, the latter concern is essential to obtain precise measurements. Consequently, studying the MTS using both measurement configurations is extremely useful, above all when evaluating the absorption of a MTA, aiming to reduce the Radar Cross Section (RCS) of certain objects.

A. Quasi-monostatic measurements of the Pilar MTA

The guidelines presented in [14] will be applied in this paper to improve the quasi-monostatic set-up and retrieve more precise results. In the cited paper, it was concluded that a proper orientation of the antennas pointing to the MTS, a compromise between the MTS size and the distance to meet the far-field condition and an optimum antennas arrangement to couple as much transmitted field as possible on the MTS and at the same time avoiding the coupling between the antennas, is crucial to obtain accurate measurements. In this paper, apart from the previous factors, other ones are examined aiming at further improving the measurement results. Consequently, the following additional considerations are taken into account:

- The calibration prototype (metallic plate) and the MTA measurements are acquired at smaller angular steps, so that a more precise correction of the positioning misalignments of both structures can be applied on the post-processing stage. In [14], the MTA is rotated with a 2º difference between consecutive measurements, in this case this resolution is increased to 0.5º.
- Several measurements are recorded for each angular position of the MTA, in order to test the measurement repeatability and apply proper data processing to reduce the receiver noise.
- Measurements of the set-up are conducted before and after measuring the MTA and the metallic plate (with an empty chamber), aiming to ensure that no other unwanted scattering echoes or instrumentation errors appear in the set-up, during the acquisition of the measurements from both structures (MTA and metallic plate).

The distance between the antennas and the MTA is 1.3m (same as in [14]) and the arrangement of the antennas, is identical to the one in which the more precise measurement results are obtained in [14]. Therefore, CONTE1 configuration (see the cited reference) is used for measuring the MTA under TE polarization, with a horizontal separation between antennas of 35cm. For TM polarization, the distance between the antennas will be fixed to be 27 cm in the vertical axis. The scattering patterns of the metallic plate and the MTA are recorder at the resonance frequency of the latter and the slight misalignments on the positioning are adjusted. Furthermore, a proper corrected measurement reference (CMR) is defined analogously to [14], for each set-up configuration. Following the previous advice, quasi-monostatic measurements are conducted under both TE and TM polarizations and presented in Fig. 1 and Fig. 2, respectively. Moreover, TABLE I. and 0compare the measurements conducted following the recommendations presented in [14] with the new ones introduced here (which also consider [14]), regarding the resonance frequency (f_r), absorption peak (*AP*) and the full width at half maximum (*FWHM*). As it can be observed from the tables, similar resonance frequencies are obtained, which is logical since the MTA resonance only changes when its inclusions are modified. However, the measurements presented in this paper exhibit a closer *AP* values to the simulations ones (see [16]). On the other hand, it should be mentioned that the FWHM is slightly broader in the presented measurements than in [14]. Indeed, for both measurements, it is a bit larger than in simulation (2%). The latter can be attributed to the blueshift of the resonance frequency as compared to simulations, which as lies at a higher frequency may exhibit a broader bandwidth (this is related to the MTA quality factor). Moreover, it should be noticed that the FWHM is a relative measurement depending on the *AP* value, which slightly varies from simulation to measurement.
Consequently, although the measurable angular margin is not considerable increased from the already presented measurements in [14] (just an additional angle for TE could be measured), the measured absorption values shown in this paper approach in a greater extent to the ones obtained in simulation. Therefore, the new guidelines introduced here are useful to improve the measurement accuracy.

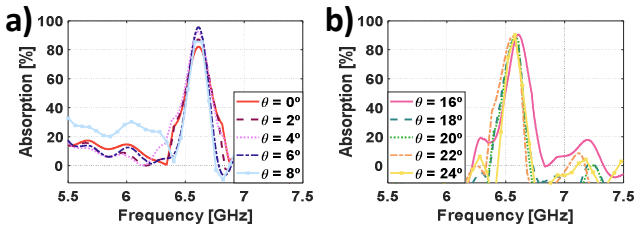

Fig. 1. Quasi-monostatic measurement of the MTA absorption under TE polarization for incidence angles from 0º to 8º (a) and 16º to 24º (b).

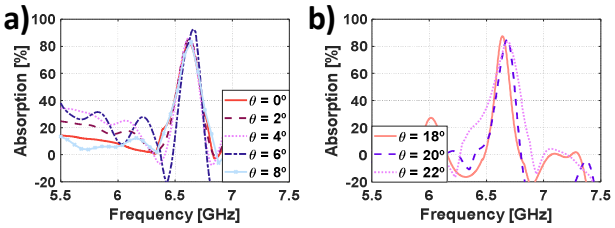

Fig. 2. Quasi-monostatic measurement of the MTA absorption under TM polarization for incidence angles from 0º to 8º (a) and 18º to 22º (b).

TABLE I. QUASI-MONOSTATIC MEASUREMENT COMPARISON UNDER TE POLARIZAITON

Incidence angle (º)	Previous paper [14]			Current paper		
	f_r (GHz)	*AP* (%)	*FWHM* (%)	f_r (GHz)	*AP* (%)	*FWHM* (%)
0º	6.62	73.36	2.14	6.61	82.13	4.18
2º	6.62	70.58	2.18	6.61	87.29	4.03
4º	6.62	69.61	2.42	6.61	92.44	3.87
6º	6.62	69.83	2.84	6.61	95.69	3.03
8º	6.62	66.63	2.99	6.61	91.28	2.94
10º	6.61	72.37	-	-	-	-

Incidence angle (º)	Previous paper [14]			Current paper		
	f_r (GHz)	AP (%)	FWHM (%)	f_r (GHz)	AP (%)	FWHM (%)
12º	6.62	76.01	-	-	-	-
16º	6.61	59.89	1.66	6.61	90.43	3.63
18º	6.61	68.63	1.78	6.57	87.45	3.68
20º	6.6	76.28	1.94	6.58	88.84	3.59
22º	6.59	76.12	2.15	6.56	89.27	3.69
24º	-	-	-	6.57	87.06	2.68

TABLE II. QUASI-MONOSTATIC MEASUREMENT COMPARISON UNDER TM POLARIZAITON

Incidence angle (º)	Previous paper [14]			Current paper		
	f_r (GHz)	AP (%)	FWHM (%)	f_r (GHz)	AP (%)	FWHM (%)
0º	6.62	61.34	2.9	6.62	82.11	3.69
2º	6.62	62.21	3.11	6.62	85.66	3.44
4º	6.62	63.97	2.93	6.62	86.41	3.2
6º	6.62	66.39	3.14	6.66	92.5	2.97
8º	6.61	66.77	2.99	6.63	84.01	3.53
10º	6.6	61.83	2.27	-	-	-
18º	6.68	49.88	1.35	6.64	87.42	2.17
20º	6.7	61.64	1.85	6.68	84.9	2.6
22º	6.7	59.41	2.09	6.69	83.38	4.13

B. *Bistatic measurements of the Pilar MTA*

The set-up for conducting bistatic measurements is arranged as it is shown in Fig. 3. The transmitting and receiving antennas are shifted along the low-reflecting bench (represented in orange in the picture) to impinge on the MTA at different incidence angles. It should be mentioned that the receiving antenna under TM configuration is at a smaller height than the transmitting one in order to avoid coupling between them. Moreover, for both polarizations, the antennas are reoriented in each position, so that they point to the MTA. A metallic plate with identical dimensions to the MTA will be used for calibration purposes.

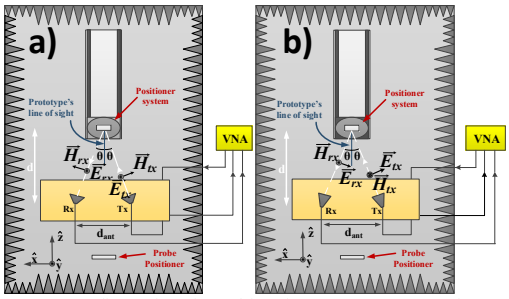

Fig. 3. Set-up configuration for a bistatic measurement under TE (a) and TM (b) polarization.

The measurement results are shown in Fig. 4 and more meticulously in TABLE III. It should be noticed that bigger prototypes need a longer distance to meet the far-field condition and hence, higher separation between antennas are required to impinge on the MTA at large incidence angles. In this case, the MTA is measured at 1.3m and the maximum distance between the transmitting and receiving antennas is determined by the anechoic chamber width, the possibility of properly focusing the incident field on the MTA and the length of the available low-reflecting benches, which is 2m. In this case, the latter will determine the angular margin that can be measured. Considering the previous restriction, the maximum angle at which the MTS can be experimentally characterized is 38º $\left(\tan^{-1}(1/1.3)\right)$. Larger angles can be obtained if longer benches were available, however, there could be difficulties on focusing the incident wave on the MTA. Indeed, as it can be seen from the TE polarization measurements, the one conducted at 38º exhibits high scattering values (Fig. 4 (a)).

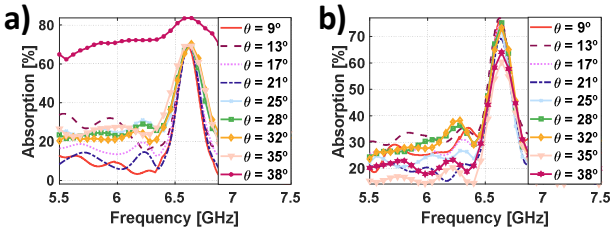

Fig. 4. Bistatic measurement of the MTA absorption under TE (a) and TM (b) polarization.

TABLE III. BISTATIC MEASUREMENT RESULTS

Incidence angle (º)	TE			TM		
	f_r (GHz)	AP (%)	FWHM (%)	f_r (GHz)	AP (%)	FWHM (%)
9º	6.61	68.92	3.48	6.63	76	4.31
13º	6.62	69.77	3.87	6.62	77.04	4.86
17º	6.62	69.26	3.87	6.62	74.5	4.38
21º	6.62	69.62	3.6	6.63	69.22	4.28
25º	6.62	70.22	4.77	6.63	73.05	3.98
28º	6.62	70.16	5.02	6.64	75.35	4.37
32º	6.64	70.33	5.3	6.64	73.3	4.67
35º	6.61	70.91	5.8	6.64	60.48	4.85
38º	6.61	83.85	-	6.64	64.13	5.21

III. COMPARISON BETWEEN QUASI-MONOSTATIC AND BISTATIC MEASUREMENTS

After introducing the measurements of the MTA under different incidence angles for both quasi-monostatic and bistatic set-up configurations, several conclusions can be drawn.

- For the considered MTA dimensions and range of frequencies, the MTA can be measured under larger incidence angles when using a bistatic set-up configuration.
- Similar values of resonance frequency and bandwidth were obtained using both set-ups configurations. However, higher absorption peaks (APs) were acquired under the quasi-monostatic measurement. The latter can be attributed to the receiving antenna position on the bistatic measurement set-up, which may not be exactly at the specular direction. In fact, although the measurements are retrieved for different angles at each antennas

position (by slightly moving the positioner system), small errors in placing the antennas are unavoidable. It should be noticed that positioning the antennas in this set-up is especially difficult, since the antennas are moved by hand using just a ruler as a reference and a laser level (for orienting the antennas facing the MTA).

- The angular margin is determined by the scattering pattern of the MTA and hence, by its size when a quasi-monostatic measurement is used. For the bistatic measurement, this margin is fixed by the anechoic chamber width and the possibility of properly orienting the antennas facing the MTA.
- Post-processing is crucial to adjust slight misalignments between the position of the MTA and the reference metal plate.

IV. CONCLUSIONS

In the presented paper, a metasurface absorber has been experimentally characterized inside an anechoic chamber under both quasi-monostatic and bistatic set-up configurations. More precise quasi-monostatic measurements to the ones introduced in [14] has been presented following the mentioned additional considerations. The limitations of characterizing MTS using both set-up configurations have been shown, as well as a comparison between them. Moreover, several conclusions have been outlined along the paper, regarding the comparison of the simulations of the infinite metasurface with the measurement of the finite one. From the results, it can be highlighted that both quasi-monostatic and bistatic measurements are greatly important to fully characterize the MTS. Finally, it has to be stated that characterizing MTSs are not a trivial issue and an accurate set-up arrangement and a careful post-processing of the measured data is needed to obtain precise results.

ACKNOWLEDGMENT

This work was supported by the Gobierno del Principado de Asturias under Project GRUPIN18-000191 and under grant BP16024.

REFERENCES

[1] T. M. Kollatou, A. I. Dimitriadis, N. V. Kantartzis, M. Hinaje and C. S. Antonopoulos, "A class of multi-band, polarization-insensitive, microwave metamaterial absorbers in EMC analysis," International Symposium on Electromagnetic Compatibility - EMC EUROPE, Rome, 2012, pp. 1-4.

[2] L. Li, J. Wang, H. Du, J. Wang, S. Qu and Z. Xu, "A band enhanced metamaterial absorber based on E-shaped all-dielectric resonators," in AIP Advances, vol. 5, no. 1, 017147, 2015.

[3] H. Luo, Y.Z. Cheng and R.Z. Gong, "Numerical study of metamaterial absorber and extending absorbance bandwidth based on multi-square patches," in The European Physical Journal B, vol. 81, no. 4, pp. 387-392, 2011.

[4] S. A. Tretyakov and S.I. Maslovski, "Thin absorbing structure for all incidence angles based on the use of a high□impedance surface," in Microwave and Optical Technology Letters, vol. 38, no. 3, pp. 175-178, 2003.

[5] A. Kazemzadeh and A. Karlsson, "Multilayered wideband absorbers for oblique angle of incidence," in IEEE Transactions on Antennas and Propagation, vol. 58, no. 11, pp. 3637-3646, 2010.

[6] M. Luo, Y. Zhou, S. Wu and L. Chen, "Wide-angle broadband absorber based on one-dimensional metasurface in the visible region," in Applied Physics Express, vol. 10, no. 9, 092601, 2017.

[7] S. Fan and Y. Song, "UHF metamaterial absorber with small-size unit cell by combining fractal and coupling lines," in International Journal of Antennas and Propagation, vol. 2018, Article ID 9409152, 9 pages, 2018.

[8] L.L. Cong, X.Y. Cao, T. Song, J. Gao and J.X. Lan, "Angular-and polarization-insensitive ultrathin double-layered metamaterial absorber for ultra-wideband application," in Scientific reports, vol. 8, no. 1, 9627, 2018.

[9] W. Xin, Z. Binzhen, W. Wanjun, W. Junlin and D. Junping, "Design and characterization of an ultrabroadband metamaterial microwave absorber," in IEEE Photonics Journal, vol. 9, no. 3, pp. 1-13, 2017.

[10] J.Q. Feng, W.D. Hu, Q.L. Zhang, H. Zong, H. Huang, Y.T. Jin and L.M. Si, "Polarization-independent and angle-insensitive metamaterial absorber using 90-degree-rotated split-ring resonators," International Journal of Antennas and Propagation, vol. 2015, Article ID 240691, 6 pages, 2015.

[11] D. Sood and C.C. Tripathi, "Broadband ultrathin low-profile metamaterial microwave absorber," in Applied Physics A, vol. 122, no. 4, pp. 332, 2016.

[12] D. Lee, J.G. Hwang, D. Lim, T. Hara and S. Lim, "Incident angle-and polarization-insensitive metamaterial absorber using circular sectors," in Scientific reports, vol. 6, 27155, 2016.

[13] V.L. Mol and C.K. Aanandan, "An ultrathin microwave metamaterial absorber with enhanced bandwidth and angular stability," in Journal of Physics Communications, vol. 1, no. 1, 2017.

[14] H. Fernandez Alvarez, M. E. de Cos Gomez and F. Las-Heras, "Angular Stability of Metasurfaces: Challenges Regarding Reflectivity Measurements [Measurements Corner]," in IEEE Antennas and Propagation Magazine, vol. 58, no. 5, pp. 74-81, Oct. 2016.

[15] F. Capolino, Theory and phenomena of metamaterials. CRC press, 2009.

[16] H. Fernandez Alvarez, M.E. de Cos and F. Las-Heras, "A Six-Fold Symmetric Metamaterial Absorber. Materials," vol. 8, no. 4, pp. 1590-1603, 2015.